Working draft of the Manuscript about Viscoelastic Migration of a rigid sphere (both Forced and Force-free)

1 Inertial Migration

1.1 Introduction

Nice progress!

As per the properties of the Stokes flow, in the absence of inertia (i.e., Stokes regime), a rigid sphere cannot migrate across streamlines due to the reversibility of the Stokes flow; however, cross-stream migration is observed in several experiments. Therefore, cross-stream migration is attributed to fluid inertia. The Segre-Silberberg effect of inertia-induced lateral migration also shows that the spheres reach a stable lateral equilibrium position independent of the initial position of release (for poiseuille flow its **0.6R** where R is the radius of pipe.

1.1.1 Background flow Field

For poiseuille flow the full dimensionless governing equations and boundary conditions for the velocity and pressure fields U and P expressed in the particle frame of reference where **V** represents the dimensionless undisturbed bulk flow while V_{w} ,is the dimensionless velocity of the walls.

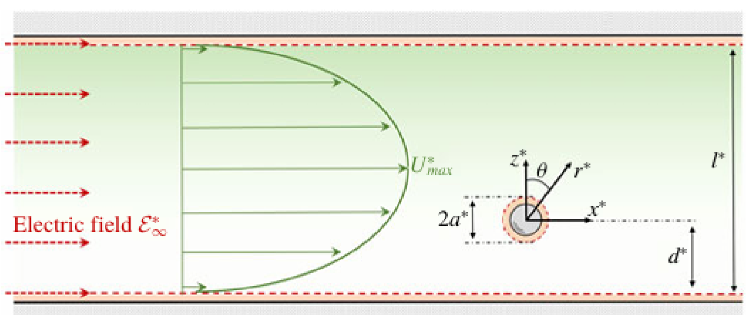

Figure 1: Schematic of the problem formulation. The origin of the coordinate system is at the centre of the particle. Here, y points in the direction of vorticity of the pressure driven flow. The dashed layer around the particle and walls depicts the outer edge of the double layer. Here, * denotes the dimensional variables.

$$\begin{aligned} \nabla^2\mathbf{U} - \nabla P = Re(\mathbf{U}\cdot\nabla)\mathbf{U}, \quad \nabla\cdot\mathbf{U} = 0, \\ \mathbf{U} = \mathbf{\Omega}_s \times \mathbf{r} \quad \text{on } r = 1, \\ \mathbf{U} = \mathbf{V}_w - \mathbf{U}_s \quad \text{on the walls}, \\ \mathbf{U} \to \mathbf{V} \quad \text{as } r \to \infty. \end{aligned} \tag{1}$$

Solution of the governing equation using the desired boundary conditions for a Poiseuille flow we get the dimensionless Undisturbed velocity profile as follows:

$$\mathbf{V} = (\alpha + \beta z + \gamma z^2)\mathbf{e}_x - \mathbf{U}_s, \quad Q = 2\gamma x, \tag{2}$$

Where:

$$\alpha = \frac{4s(1-s)}{\kappa}, \quad \beta = 4(1-2s), \quad \gamma = -4\kappa$$

here α is the linear velocity term, β represents the shear component and γ contains the curvature of the background undisturbed flow. κ is the ratio of the particle radius a and l is width of the channnel. Since the migration occurs due to weak inertia, the migration velocity is much smaller than the characteristic velocity, which suggests that we can neglect the temporal variations. Therefore, the velocity and pressure distribution in the bulk are governed by continuity and quasi-steady Navier–Stokes equation.

1.1.2 Disturbance velocity

Introducing the governing equations and boundary conditions for disturbance velocity fields

$$\begin{gathered}
\nabla^2 \mathbf{v} - \nabla q = Re\left(\mathbf{v}\cdot\nabla\mathbf{v} + \mathbf{v}\cdot\nabla\mathbf{V} + \mathbf{V}\cdot\nabla\mathbf{v}\right), \\
\nabla\cdot\mathbf{v} = 0, \\
\mathbf{v} = \mathbf{\Omega}_s \times \mathbf{r} - \mathbf{V} \quad \text{on } r = 1, \\
\mathbf{v} = 0 \quad \text{on the walls}, \\
\mathbf{v} \to 0 \quad \text{as } r \to \infty.
\end{gathered} \tag{3}$$

Here the inertia term vanishes because we have considered unidirectional flow. Also, the particle Reynold's number based on the average shear rate for two dimensional poiseuille flow will be $Re = \rho_0 V'_{max}\kappa a/\mu_0$ and its found out that $Re << \kappa^2$, that is viscous stresses dominate throughout the channel.Actually, the condition $Re << \kappa^2$ implies that $Re << 1$.

1.2 Solution Techniques/Approach

Following the Cox & Brenner approach of asymptotic expansion for the disturbance velocity fields and pressure fields $\mathbf{v}$ and $\mathbf{q}$ in which the individual terms $(\mathbf{v}^{(0)}, \mathbf{q}^{(0)})$ and $(\mathbf{v}^{(1)}, \mathbf{q}^{(1)})$ satisfy the above equations. At present, we are interested in calculating the lateral migration velocity $U_{sz}^{(1)}$, which is the z component of $\mathbf{U}_s^{(1)}$. Clearly, $\mathbf{U}_{sz}^{(1)}$ could be determined by solving for $\mathbf{v}^{(1)}$ leaving $\mathbf{U}_s^{(1)}$ and $\mathbf{\Omega}_s^{(1)}$ unspecified and then applying the conditions of zero net external force and torque on the freely suspended particle; however, it can be shown that a complete solution for $\mathbf{v}^{(1)}$ is not necessary for this purpose. Instead, a version of the well-known **Lorentz reciprocal theorem** can be employed; this allows the migration velocity to be expressed in terms of a certain volume integral over the total fluid volume.

For LRT we have to define a test velocity field so let's take it ($\mathbf{u}$,p), it is the velocity field for a sphere translating with unit velocity perpendicular to the walls in a quiescent fluid. As per **LRT** we can write the relation of the first reflection of the disturbance velocity field and the test field.

$$(\nabla\cdot\boldsymbol{\tau}^{(\mathbf{1})} - \mathbf{f})\cdot\mathbf{u} = 0, \quad (\nabla\cdot\mathbf{t})\cdot\mathbf{v}^{(\mathbf{1})} = 0 \tag{4}$$

Where, $\boldsymbol{\tau}^{(\mathbf{1})}$ and $\mathbf{f}$ are:

$$\boldsymbol{\tau}^{(\mathbf{1})} = -q^{(1)}\mathbf{I} + \nabla\mathbf{v}^{(\mathbf{1})} + (\nabla\mathbf{v}^{(\mathbf{1})})^T, \tag{5}$$

$$\mathbf{f} = \mathbf{v}^{(\mathbf{0})}\cdot\nabla\mathbf{v}^{(\mathbf{0})} + \mathbf{v}^{(\mathbf{0})}\cdot\nabla\mathbf{V} + \mathbf{V}\cdot\nabla\mathbf{v}^{(\mathbf{0})} \tag{6}$$

From this we can easily derive the inertia-induced force which is given by:

$$F_L = -Re\int_{Vf}(\mathbf{f}\cdot\mathbf{u})dV \tag{7}$$

The function $\mathbf{f}$ can bre determined completely once the term $\mathbf{v}^{(\mathbf{0})}$ is available and the solution of the test field is straightforward. Therefore, the **LRT** offers a considerably simplified scheme for calculating the lateral migration velocity,especially when compared with the alternative to solve the full first order velocity field $\mathbf{v}^{(\mathbf{1})}$.

1.3 Results and discussion

As we have seen, the corresponding velocity field $\mathbf{v^{(0)}}$ is required to evaluate F_L using the reciprocal theorem, equation (7), the solution of this is found by means of the iterative method of reflexions in which the complete solution $\mathbf{v^{(0)}}$ is constructed as a sum of terms which alternatively satisfy boundary conditions on the surface of the sphere and on the walls. Now, since $\mathbf{v^{(0)}}$ satisfies the boundary conditions so its reflections $\mathbf{v_1^{(0)}}$ will also satisfy the boundary conditions. Hence, the solution of $\mathbf{v_1^{(0)}}$ is found out by using the general **Lamb's solution**. Similarly, the first reflection test field $\mathbf{u}$ is also found out using the Lamb's solution.

Once both f and u are found out and we evaluate the integrand we see that it behaves as

$$\mathbf{u.f} \sim \kappa^2 O\left(\frac{1}{r^3}, \frac{1}{r^5}, \frac{1}{r^7}\right) + \kappa^3 O\left(\frac{1}{r^2}, \frac{1}{r^3}, \frac{1}{r^4}, \dots\right) + \dots. \tag{8}$$

Also if we analyze the lateral induced force, it is seen that the dominant term in the expression for neutrally buoyant particles is due to the stresslet (D1, determined by the bulk rate of strain) and its reflexion off the walls. The Stokeslet contribution (Al, originating from the lag velocity) and the couplet contribution (C1, originating from the rotation slip) are of one and three orders of magnitude smaller in κ, and hence may be neglected for this case. Therefore if we solve for the lateral migration force the integrand does not converges in the limits of $r \to [1, \infty)$.

2 Viscoelastic Migration

In the above case we evaluated the lateral migration of the rigid particles we saw that the significant migration lift force comes from the walls stresses which was also not very profound to provide lateral lift to the particle, It was for the case of Newtonian fluids.Now, it is already shown experimentally that the magnitude and direction of lateral migration in non-Newtonian liquids depend critically on the detailed rheological characteristics of the suspending fluid.

Second Order Fluids::We can visualize the main complexity in second order fluids by simply taking an example of a polymer solution, (a very common example of a non-Newtonian fluid), if we see it as a microscale a polymer chain is coiled in its lowest energy state and when its kept in flow conditions it elongates as well as deforms but tries to resist due to which two additional straining terms is seen in the stress tensor equation.
It is, of course, well known that the second-order fluid model is only relevant for very slow and thus nearly Newtonian flows. In particular, deviations of the normal stress components from their Newtonian values are strictly of only infinitesimal magnitude.
Also on briefly describing the two Normal stress differences, the first Normal stress difference is between the stress of flow direction to the stress in the velocity gradient direction which is dominant for polymer solutions which is basically a tension in the streamlines, while the second normal stress differnce is between the stress in the velocity gradient direction to the stress in vorticity direction.However, for polymers and other fibres there is no activity in vorticity direction so there is no second normal stress differences and that is the reason why N_2 is neglected.

Here,we consider a complete theoretical analysis for plane quadratic shear flow of a second order fluid.The analysis aligns with the experimental analysis and predicts that the lateral migration will occur in the same direction as observed in experiments.

2.1 Problem Formulation

We consider a neutrally buoyant rigid sphere of radius a freely suspended in an incompressible second-order fluid which is confined between two parallel plane walls separated by a distance d. Rest all the terms are same only the characteristics velocity changes from $V_{max}(a/d)$ to **Ga** where G is the average shear rate for the bulk flow. The equations of motion may thus be expressed in the form:

$$Re\left[\frac{\partial \mathbf{V}}{\partial t} + \mathbf{V} \cdot \nabla \mathbf{V}\right] = \nabla \cdot \mathbf{\Pi}, \quad \nabla \cdot \mathbf{V} = 0, \tag{9}$$

Where the stress tensor $\mathbf{\Pi}$ for a second order fluid is:

$$\mathbf{\Pi} = -P\mathbf{I} + \mathbf{E}_{(1)} + \lambda \mathbf{E}_{(1)} \cdot \mathbf{E}_{(1)} + \lambda \epsilon_1 \mathbf{E}_{(2)},$$

$$\mathbf{E}_{(1)} = \nabla \mathbf{V} + \nabla \mathbf{V}^T,$$

$$\mathbf{E}_{(2)} = \frac{\partial \mathbf{E}_{(1)}}{\partial t} + \mathbf{V} \cdot \nabla \mathbf{E}_{(1)} + \mathbf{E}_{(1)} \cdot \nabla \mathbf{V}^T + \nabla \mathbf{V} \cdot \mathbf{E}_{(1)}.$$

Where $\mathbf{E}_{(1)}$ is the rate of strain tensor and $\mathbf{E}_{(2)}$ is the actually the upper convected derivative or Oldroyd derivative of $\mathbf{E}_{(1)}$ also known as the Rivlin-Ericksen Tensor.The dimensionless parameter h is a measure of the intrinsic relaxation time for the suspending fluid relative to the dynamic scale G^{-l}. In the present work we consider $\boldsymbol{\lambda}$ to be small so that the constitutive relationship differs only slightly from that of a Newtonian fluid, the other non-Newtonian parameter ϵ_1 is the ratio of the magnitudes of normal stress components in shear flow. The case ϵ_1 = - 0.5 corresponds to the so-called Weissenberg fluid, in which the second normal-stress difference is exactly zero.

Now, Considering the undisturbed bulk flow to be steady, unidirectional and two dimensional, with a quadratic lateral variation in velocity, even when referred to convected co-ordinates fixed at the sphere center.Using these assumptions we simplify the equations and upon solving for the background flow field this time we get,

$$\mathbf{V} = (\alpha + \beta x + \gamma x^2)\mathbf{e_x} - (\mathbf{U_s})_x \tag{10}$$

$$Q = 2\gamma x + 4\gamma(\beta x + \gamma x^2)(1 + 2\epsilon_1)\lambda + \text{constant}, \tag{11}$$

here the terms α, β and γ are same as in the previous case. It may be noted that, for a second-order fluid, the undisturbed velocity field is unchanged from that of a Newtonian fluid having the same viscosity μ_0, but does produce a contribution to the isotropic pressure at order λ.
On proceeding further to calculate the disturbance velocity field $\mathbf{v}$ and pressure field $\mathbf{q}$:

$$\nabla \cdot \boldsymbol{\pi} = 0, \quad \nabla \cdot \mathbf{v} = 0, \tag{12}$$

$$\boldsymbol{\pi} = -q\mathbf{I} + \mathbf{e}_{(1)} + \lambda[\mathbf{e}_{(1)} \cdot \mathbf{e}_{(1)} + \mathbf{W}_{(1)}] + \lambda\epsilon_1[\mathbf{e}_{(2)} + \mathbf{W}_{(2)}] \tag{13}$$

where,

$$\begin{aligned} \mathbf{e}_{(1)} &= \nabla \mathbf{v} + \nabla \mathbf{v}^T, \\ \mathbf{e}_{(2)} &= \mathbf{v} \cdot \nabla \mathbf{e}_{(1)} + \mathbf{e}_{(1)} \cdot \nabla \mathbf{v}^T + \nabla \mathbf{v} \cdot \mathbf{e}_{(1)}, \\ \mathbf{W}_{(1)} &= \mathbf{E}_{(1)} \cdot \mathbf{e}_{(1)} + \mathbf{e}_{(1)} \cdot \mathbf{E}_{(1)}, \\ \mathbf{W}_{(2)} &= \mathbf{V} \cdot \nabla \mathbf{e}_{(1)} + \mathbf{e}_{(1)} \cdot \nabla \mathbf{V}^T + \nabla \mathbf{V} \cdot \mathbf{e}_{(1)} + \mathbf{v} \cdot \nabla \mathbf{E}_{(1)} + \mathbf{E}_{(1)} \cdot \nabla \mathbf{v}^T + \nabla \mathbf{v} \cdot \mathbf{E}_{(1)}. \end{aligned} \tag{14}$$

Here, $\mathbf{e}_{(1)}$ and $\mathbf{e}_{(2)}$ are the rate of strain tensor and the Rivlin Erickson Tensor respectively, While the new terms $\mathbf{W}_{(1)}$ and $\mathbf{W}_{(2)}$ are the tensors arising from the interaction of the disturbance flow velocity $\mathbf{v}$ and the background flow velocity $\mathbf{V}$. Similar to the inertial migration in case of Newtonian fluids here also we asymptotically expand the disturbance velocity and pressure fields and will obtain governing equations for $\mathbf{v}^{(0)}$ and $\mathbf{v}^{(1)}$. For ($\mathbf{v}^{(1)}$,$q^{(1)}$),we obtain:

$$\nabla \cdot \boldsymbol{\pi}^{(1)} = 0, \quad \nabla \cdot \mathbf{v}^{(1)} = 0, \tag{15}$$

$$\boldsymbol{\pi}^{(1)} = -q^{(1)}\mathbf{I} + \mathbf{e}^{(1)}_{(1)} + \mathbf{\Sigma}^{(0)}, \tag{16}$$

$$\mathbf{\Sigma}^{(0)} = \mathbf{e}^{(0)}_{(1)} \cdot \mathbf{e}^{(0)}_{(1)} + \mathbf{W}^{(0)}_{(1)} + \epsilon_1[\mathbf{e}^{(0)}_{(2)} + \mathbf{W}^{(0)}_{(2)}]. \tag{17}$$

and the appropriate boundary conditions are:

$$\mathbf{v}^{(1)} = \mathbf{\Omega}^{(1)}_s \times \mathbf{r} + \mathbf{U}^{(1)}_s \quad \text{on} \quad r = 1, \tag{18}$$

$$\mathbf{v}^{(1)} = 0 \quad \text{on the walls}, \tag{19}$$

$$\mathbf{v}^{(1)} \to 0 \quad \text{as} \quad r \to \infty. \tag{20}$$

Here $\mathbf{\Omega}_s^{(1)}$ and $\mathbf{U}_s^{(1)}$ are the angular and translational velocities of the sphere at $\mathcal{O}(\lambda)$. All of the variables $\mathbf{\Omega}_s^{(0)}$, $\mathbf{\Omega}_s^{(1)}$, $\mathbf{U}_s^{(0)}$, and $\mathbf{U}_s^{(1)}$ are unknown, in general, and must be obtained as part of the solution to the problem. Our present objective is to find the z component of $\mathbf{U}_s^{(1)}$, which is the lateral velocity of the sphere induced by the non-Newtonian behaviour of the suspending fluid. Now, following the same approach as the previous calculation and using Lorentz Reciprocal Theorem by introducing a test velocity field.A new velocity ($\mathbf{u}$,p)is defined as:

$$\nabla \cdot \mathbf{t} = 0, \quad \nabla \cdot \mathbf{u} = 0, \tag{21}$$

$$\mathbf{t} = -p\mathbf{I} + \mathbf{a}, \quad \mathbf{a} = \nabla \mathbf{u} + \nabla \mathbf{u}^{\mathrm{T}}, \tag{22}$$

Combining both the velocity fields and integrating over the entire fluid volume we get:

$$\int_{V_t} \nabla \cdot \left[\mathbf{u} \cdot \boldsymbol{\pi}^{(1)} - \mathbf{v}^{(1)} \cdot \mathbf{t}\right] dV - \int_{V_t} \left\{\boldsymbol{\pi}^{(1)} \colon \nabla \mathbf{u} - \mathbf{t} \colon \nabla \mathbf{v}^{(1)}\right\} dV = 0. \tag{23}$$

On further rearranging and on applying the Gauss-Divergence Theorem to the first integral we finally obtain the integrand which would give us the lateral migration lift force which is as follows:

$$F_L = -\frac{1}{2}\lambda \int_{V_t} \mathbf{\Sigma}^{(0)} \colon \mathbf{a}\, dV. \tag{24}$$

Note: If we compare this lift force with the force expression we got in the inertial migration problem we can notice some significant and some subtle changes In particular, equation (7) has the inhomogeneous term $\mathbf{f}$ of the $O(\mathrm{Re})$ equations of motion dotted directly with $\mathbf{u}$, whereas the present form (24) involves the double dot product of the inhomogeneous part of the stress tensor at $O(\lambda)$ with the rate-of-strain tensor corresponding to $\mathbf{u}$.

2.2 Evaluation of Lift Force

In order to evaluate the lift force F_L by integrating the double dot product ($\mathbf{\Sigma}^{(0)} \colon \mathbf{a}$) over the volume of fluid which is outside the sphere and bounded by the walls. On retracing the paths one by one we found out that $\mathbf{\Sigma}^{(0)}$ can be found out by using $\mathbf{v}^{(\mathbf{0})}$ and $\mathbf{u}$ and we already have the solution of both $\mathbf{v}^{(\mathbf{0})}$ and $\mathbf{u}$ which were derived by lamb's solution same as the inertial migration problem. The first reflection ($\mathbf{v}_{(0)}^{(1)}$, $p_{(0)}^{(1)}$) is found by employing Lamb's general solution

$$\begin{aligned}
\mathbf{v}_{(0)}^{(1)} &= A_1 \left(\mathbf{e}_x + \frac{x\mathbf{r}}{r^2}\right)\frac{1}{r} + B_1 \left(-\mathbf{e}_x + \frac{3x\mathbf{r}}{r^2}\right)\frac{1}{r^3} + C_1 \left(\frac{x\mathbf{e}_z}{r^3} - \frac{x\mathbf{e}_x}{r^3}\right) + D_1 \frac{xz\mathbf{r}}{r^5} \\
&+ E_1 \left(2\mathbf{e}_x + x\mathbf{e}_z - \frac{5xz\mathbf{r}}{r^2}\right)\frac{1}{r^5} + F_1 \left(\mathbf{e}_x - \frac{2x^2\mathbf{e}_x + x\mathbf{r}}{r^2} + \frac{2x\mathbf{e}_z}{r^2}\right)\frac{1}{r^3} \\
&+ G_1 \left(\mathbf{e}_x - \frac{5z^2\mathbf{e}_x + 10xz\mathbf{e}_z + 13x\mathbf{r}}{r^2} + \frac{75xz^2\mathbf{r}}{r^4}\right)\frac{1}{r^3} \\
&+ H_1 \left(\mathbf{e}_x - \frac{5z^2\mathbf{e}_x + 10xz\mathbf{e}_z + 5x\mathbf{r}}{r^2} + \frac{35xz^2\mathbf{r}}{r^4}\right)\frac{1}{r^5}.
\end{aligned} \tag{25}$$

$$p_{(0)}^{(1)} = A_1 \frac{3x}{2r^3} + D_1 \frac{2xz}{r^5} + G_1 \left(\frac{-30x}{r^5} + \frac{150xz^2}{r^7}\right). \tag{26}$$

Here, the coefficients are defined as

$$\begin{cases}
A_1 = \frac{3}{4}\left(U_{sx(0)} - \alpha - \frac{\gamma}{3} - Ha(\zeta_p - \zeta_w)\right), \\
B_1 = -\frac{1}{4}\left(U_{sx(0)} - \alpha - \frac{3\gamma}{5} - Ha(\zeta_p - \zeta_w)\right) + Ha\frac{\zeta_p}{2}, \\
C_1 = \Omega_{sy(0)} - \frac{\beta}{2}, \quad D_1 = \frac{5\beta}{2}, \quad E_1 = \frac{\beta}{2}, \\
F_1 = \frac{\gamma}{3}, \quad G_1 = \frac{7\gamma}{120}, \quad H_1 = \frac{\gamma}{8}.
\end{cases} \tag{27}$$

We have solved it step by step by first evaluating the rate of strain tensors and other terms in $\mathbf{\Sigma}^{(0)}$ which were $\mathbf{e}^{(0)}_{(1)}, \mathbf{W}^{(0)}_{(1)}, \mathbf{e}^{(0)}_{(2)}$ and $\mathbf{W}^{(0)}_{(2)}$ and then to get the desired integrand we double dotted it with the stress tensor of the test field ($\mathbf{a}$), here we have also transformed the coordinates from cartesian to spherical (since the lateral force is of the sphere in y direction) because the integral is over the spherical volume. Finally, we got the lateral migration force to be :

$$F_L = \frac{10}{3}\pi\beta\gamma(1 + 3\epsilon_1)\lambda \tag{28}$$

Unlike the inertial case, the reflexion of the infinite-domain solution off the walls yields only higher-order corrections to F_L. Thus, in calculating the lateral force to $O(\kappa^3)$ for a sphere not too close to a wall, the only role played by the walls is in the establishment of the undisturbed profile V. In addition, it should be noted from (25) that the lateral force F_L is proportional to $\beta\gamma$. Hence in the case of simple shear ($\gamma = 0$) no lateral migration will occur to $O(\kappa^3)$.

2.3 Some Important Observations

It is observed that the lateral force has the contribution of only $\mathbf{W}^{(0)}_{(1)}$ and $\mathbf{W}^{(0)}_{(2)}$ while the contribution of the other two terms ($\mathbf{e}^{(0)}_{(1)} \cdot \mathbf{e}^{(0)}_{(1)}$ and $\mathbf{e}^{(0)}_{(2)}$) is zero. Also, we already know that the lateral force for a neutrally buoyant sphere with no external torque in the inertial case is due to the stresslet caused by wall stresses.But, here in the non-Newtonian case, the lateral force depends on the disturbance velocity field close to the sphere and its seen that all the coefficient terms in the lamps solution of $\mathbf{v^{(0)}}$ contribute the same order of magnitude. However, the contributions from the Stokeslet term A, and the rotlet term C, are asymptotically small and thus neglected for a neutrally buoyant, freely rotating particle.

On comparing with the order of magnitude analysis we have shown it earlier that lateral force due to inertial contribution is of order $Re\kappa^2$ while the lateral force in the viscoelastic fluid is of order $\lambda\kappa^3$.Thus, now $Re << \lambda << 1$ can be more precisely written as $Re << \lambda\kappa$. Finally, the obtained expression of F_L is strictly negative for $\lambda > 0$ and $\epsilon_1 < -0.5$ this implies that the particle will migrate in the direction of least shear rate.Thus the equilibrium position of particles in Poiseuille flow is midway between the walls.

3 Electrokinetically influenced Visoelastic Migration

We have observed that there is a significant lift force in the case of neutrally buoyant viscoelastic migration, Now in this section we will investigate the effects of electrokinetics on the particle which is migrating in the same viscoelastic fluid where electric field is applied parallel to the flow.Here, also we will follow the same approach of using the Reciprocal Theorem and will obtain the lift force and will see an enhancement in migration to that of a neutrally buoyant particle in viscoelastic flow. We are majorly interested in the electrophoretic mobility relation with the zeta potential for a particle in the viscoelastic flow and for this problem statement the we have assumed the particle has thin debye layer which would replicate our desired case perfectly.

3.1 Problem Formulaton

We consider the same case but since there is an external electric field applied parallel to the flow and the fluid is viscoelastic so we have a new characteristic term for non-dimensionalizing electric potential which is $\mathcal{E}^*_\infty$ and rest all parameters such as velocity, dynamic viscosity, particle radius and channel width same as the viscoelastic migration as well as inertial migration problem here also we assume $\kappa << 1$ where κ is the ratio of particle radius to the channel width. The potential (ψ) in the electroneutral bulk region is governed by the Laplace equation:

$$\nabla^2\psi = 0 \tag{29}$$

and the boundaqry conditions are:

$$e_r \cdot \nabla\psi = 0 \quad \text{at } r = 1 \quad \text{and} \quad e_z \cdot \nabla\psi = 0 \quad \text{at } z = -\frac{s}{\kappa} \text{ and } z = \frac{1-s}{\kappa}, \tag{30}$$

where $s \equiv d^*/l^*$ (as defined in figure **2**). The potential is undisturbed ($\phi_\infty \sim -x$) far away from the particle $\phi \to \phi_\infty \quad \text{as} \quad r \to \infty$.

The hydrodynamics governing equations is same as the viscoelastic migration case but in order to account for the electrokinetic effects in the EDL, we employ the slip-boundary condition and impose at the particle surface so the boundary condition will change and is expressed as :

$$U = \mathbf{\Omega}_s \times r + Ha\zeta_p\nabla\phi \quad \text{at } r = 1. \tag{31}$$

$$U = Ha\zeta_p\nabla\phi - U_s \quad \text{at walls.} \tag{32}$$

Here, ζ_p is the dimensionless particle surface zeta potential $\left(\zeta_p^*/|\mathcal{E}_\infty^*|a^*\right)$ and Ha is a **Hartmann number**, $Ha = \frac{\varepsilon^*\mathcal{E}_\infty^{*2}a^*}{4\pi\mu^*\kappa U_{\max}^*}$, which denotes the ratio of electrical energy density to shear stress. Here, ε^* is the electrical permittivity of the medium. Similarly, the flow satisfies the Smoluchowski slip condition at the walls.

In the absence of particle, the flow profile for a fully developed pressure driven second-order fluid flow (in the frame of reference of the particle moving with $\mathbf{U_s}$ is:

$$U_\infty = (\alpha + \beta z + \gamma z^2)e_x + Ha\zeta_w\nabla\phi_\infty - U_s. \tag{33}$$

However, the pressure exhibits a variation in the lateral direction for SOF

$$P_\infty = 2\gamma x + 4\lambda(1 + 2\delta)(\beta z + \gamma z^2) \tag{34}$$

Same as the undisturbed background flow the disturbance flow velocity field also has the same governing equation as viscoelastic migration (eqn.12 and 13) but due to the influence of the electrokinetic behviour the new boundary conditions are:

$$\mathbf{v} = \mathbf{\Omega}_s \times \mathbf{r} + Ha\zeta_p\nabla(\psi + \phi_\infty) - \mathbf{U}_\infty \quad \text{at } r = 1 \tag{35}$$

$$\mathbf{v} = Ha\zeta_w\nabla\psi \quad \text{at walls,}$$

$$\mathbf{v} \to \mathbf{0} \quad \text{as } r \to \infty.$$

On proceeding with the perturbation expansion to calculate the first two reflections of disturbance velocity field. For small values of λ the disturbance field variables are expanded and the reflections also satisfy the governing equation. Since the electrostatic potential is decoupled from the hydrodynamics, the variable ψ is not expanded asymptotically. Hence, we obtain the problem at O(1) as:

$$\begin{cases} \nabla \cdot \mathbf{v}_{(0)} = 0, \\ \nabla^2\mathbf{v}_{(0)} - \nabla P_{(0)} = 0, \\ \mathbf{v}_{(0)} = \mathbf{\Omega}_{s(0)} \times \mathbf{r} + Ha\zeta_p\nabla(\psi + \phi_\infty) - \mathbf{U}_{\infty(0)} \quad \text{at } r = 1, \\ \mathbf{v}_{(0)} = Ha\zeta_w\nabla\psi \quad \text{at walls,} \\ \mathbf{v}_{(0)} \to \mathbf{0} \quad \text{as } r \to \infty. \end{cases} \tag{36}$$

and at $O(\lambda)$:

$$\begin{cases} \nabla \cdot \mathbf{v}_{(1)} = 0, \\ \nabla^2\mathbf{v}_{(1)} - \nabla P_{(1)} = -\nabla \cdot \mathbf{\Sigma}_{(0)}, \\ \mathbf{v}_{(1)} = \mathbf{U}_{r(1)} + \mathbf{\Omega}_{s(1)} \times \mathbf{r} \quad \text{at } r = 1, \\ \mathbf{v}_{(1)} = \mathbf{0} \quad \text{at walls,} \\ \mathbf{v}_{(1)} \to \mathbf{0} \quad \text{as } r \to \infty. \end{cases} \tag{37}$$

By the symmetry of Stokes flow we know that the zeroth reflection which is of O(1) cannot produce a lateral lift. Therefore, the lift must arise from the $O(\lambda)$ field and hence we use Reciprocal theorem to find the lift force associated to the migration velocity $\mathbf{v}_{(1)}$. The lateral lift force F_L can be evaluated using eqn.(24).

3.2 Lateral Lift Force

To estimate the migration lift force using (24), we substitute the velocity field $\mathbf{v}_{(0)}$ into the integrand:

$$F_L = 6\pi(1 + O(\kappa))U^H_{mig} = -\frac{\lambda}{2}\int_{V_1:r=1}^{r=\infty} \boldsymbol{\Sigma}_{(0)} : \mathbf{a}\, dV + o(\kappa) \tag{38}$$

On integrating and evaluating the integrand under this sub-domain we get the final layteral lift force to be:

$$F_L \approx \frac{10\pi}{3}\beta\gamma\lambda(1 + 3\epsilon_1) - \frac{3\pi}{2}\beta\lambda Ha\zeta_p(1 + \epsilon_1). \tag{39}$$

The details of $o(\kappa)$ error incurred while approximating the upper limit of the integral to $r \to \infty$ in . The order of magnitude of the leading-order disturbance,test field velocity and the undisturbed velocity are:

$$v_{(0)} \sim Ha\zeta_p O(1/r^3) + \beta O(1/r^2) + \beta O(1/r^4) + \gamma O(1/r^3) + \gamma O(1/r^5) \tag{40}$$

$$u^t \sim O(1/r) + O(1/r^3).$$

$$U_{\infty(0)} \sim \beta O(r) + \gamma O(r^2) + Ha\zeta_p O(1) + \gamma O(1).$$

3.3 Observations

In the expression of the lateral lift force eqn.(39) if we analyse it properly by the order of magnitude analysis we can clearly see that the first term is identical to that of the lateral force in neutrally buoyant viscoelastic migration of a particle in the absence of the electrokinetic effects and is of order $O(\kappa)$ while the second term which is of order O(1) has a dominant contribution in the particle migration.The expression for the migration velocity and lift force (eqn.38) shows that the direction of lateral migration is determined by the magnitude and sign of the viscometric parameter and λ. For most viscoelastic fluids λ is positive, and ϵ_1 is reported to be between -0.5 and -0.7. Since $\gamma$is negative, the first term in (38) is strictly positive below the centreline (β¿ 0) and negative above it (β¡ 0), i.e. the pure elastic stresses push the particle towards the channel axis at $O(\kappa)$. The second term is O(1), its proportionality to Haζ_p indicates that this dominant contribution originates due to the electrophoretic slip, i.e. incorporation of electrophoresis enhances the migration by $O(\kappa^{-1})$.

4 Forced Migration (Sedimentation)

In the three cases we have discussed above it was all about a neutrally buoyant (force-free) particle but in this case of a sedimenting particle there are some major changes and there is an influence due to gravity. Effects of boundaries on interfacially driven motions of particles are considerably weaker than for movement by body forces such as gravity, hence in the absence of boundaries, electrophoretic motion corresponding to such particles can be viewed as 'force-free' and is fundamentally different from the motion associated with sedimentation. Figure 2 shows the disturbance a particle creates in a quiescent fluid when subjected to these two mechanisms. The force-free electrophoretic particle motion occurs due to slipping of counter-ions over its surface. The associated disturbance field is governed by a rapidly decaying source-dipole field $O(1/r^3)$. However, the disturbance field generated from the motion induced due to density difference (buoyancy-induced motion), on the contrary, is a Stokeslet at the leading order (flow field generated due to point force), which decays significantly slower $O(1/r)$.This Stokeslet upon interaction with the background shear gives rise to a buoyancy combined inertial migration.

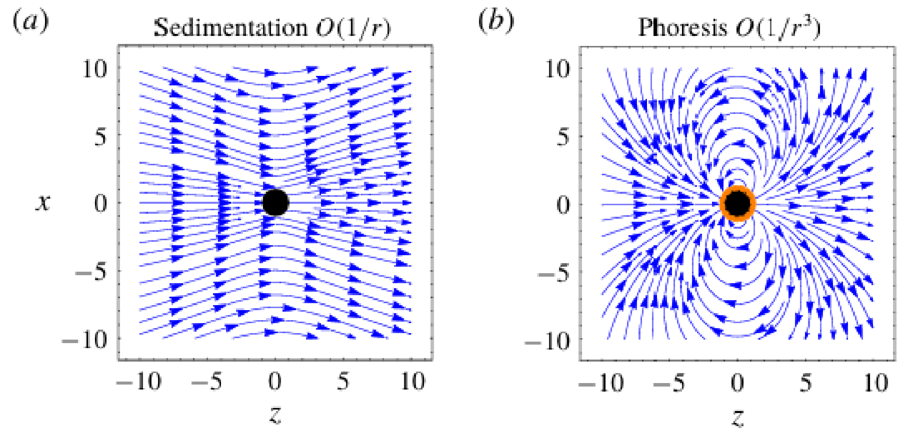

Figure 2: Disturbance velocity fields around the particle in a quiescent fluid for movements due to (a) forced (sedimentation) and (b) force-free (phoresis) mechanisms. The external field is applied in the horizontal direction.

4.1 Buoyancy combined inertial lift

In the previous section, we analysed the influence on the inertial lift due to an external field, which makes the particle lag or lead the flow via a 'force-free mechanism'. We now focus our attention on the inertial lift experienced by a non-neutrally buoyant inert particle suspended in Poiseuille flow. The gravitational field acts parallel to the flow and makes the particle lag/lead via a 'forced mechanism'. The associated disturbance profile is fundamentally different from the force-free scenario. Therefore,we focus on the influence of these differences on particle migration.

On solving the governing equations of the undisturbed flow field $U_S^{(0)}$ and the rotational velocity $\Omega_S^{(0)}$ using the lambs solution and neglecting the wall stresses we get:

$$U_S^{(0)} = \alpha + \frac{\gamma}{3} + \mathcal{B}, \quad \Omega_S^{(0)} = \frac{\beta}{2} \tag{41}$$

Here $\mathcal{B}$ is the Buoyancy number which is defined as the ratio of buoyancy force to viscous drag force:

$$\mathcal{B} = \frac{\Delta\rho^* \left(\frac{4\pi a^{*3}}{3}\right) g^*}{6\pi\mu^* a^* U^*_{max}\kappa}. \tag{42}$$

Where, ρ^* is the density difference between the particle and fluid medium and g^* is the acceleration due to gravity.

In the electrokinetically driven particle migration case, we analysed the effect of electrophoresis on the inertial migration for $Ha\zeta_p \sim O(1)$. The corresponding electrophoretic velocity was of the order of the characteristic velocity i.e. $O(U_E^*) \sim O(\kappa U_{max}^*)$. For an equitable comparison, we choose the buoyancy number ($\mathcal{B}$) to be such that the lag/lead produced by the density difference is of the same order as that in the electrophoretic system; $\mathcal{B} \sim O(1)$ corresponds to the settling velocity of the sphere being of the order of the characteristic velocity ($U_{set}^* \sim \kappa U_{max}^*$). Here U_{set}^* is the settling velocity corresponding to $\mathcal{B}$.

Using the first reflection of velocity from the lamb's solution and evaluate the integrand to find the lift force and hence the migration velocity for the case of non-neutrally buoyant particle in a viscoelastic flow. We finally found the lift force F_L to be as follows:

$$F_L \approx -\frac{\lambda}{3}\pi\beta(9\mathcal{B} - 10\gamma)(1 + 3\epsilon_1) \tag{43}$$

4.2 Observations

On analyzing the lateral lift force for the forced migration we see that the leading order of F_L is O(1) since γ is of $O(\kappa^2)$ therefore the buoyancy number in the lift force expression is a dominant parameter (assuming the usual case of λ to be positive and ϵ_1 lies between -0.5 to -0.7) and plays a significant role in the lateral migration of a non-neutrally buoyant particle in a viscoelastic fluid. Also if we during the evaluation of the integrand we can see that the buoyancy component is contributed by both the terms $\mathbf{W}_{(1)}^{(0)}$ and $\mathbf{W}_{(2)}^{(0)}$, similar to the viscoelastic migration case both the quadratic term and the corotational term of the stress tensor ($\mathbf{e}_{(1)}^{(0)} \cdot \mathbf{e}_{(1)}^{(0)}$ and $\mathbf{e}_{(2)}^{(0)}$) does not contribute to the migration velocity and the lift force. If the ratio of settling velocity to the background flow is asymptotically large (i.e. $U'_{set} \gg U'_{max}$), only the Stokeslet-wall force (SWF$_G$) exists. This corresponds to a sedimentation of a particle in a quiescent fluid ($\beta \equiv 0$ and $\gamma \equiv 0$). The particle would focus at the centreline for both positive and negative density differences (as SWF$_G$ is proportional to $\mathcal{B}^2$).

5 Particle Trajectories

In order to visualize the intensity of the migration velocity and its direction its necessary to calculate the particle trajectories. To achieve this we use the dimensional equation for the lateral velocity:

$$(U_s^*)_{mig} = \left(\frac{ds}{dt^*}\right) = \frac{-80V_{\max}^{*3}\lambda\kappa^5\left(\frac{1}{3} + \epsilon_1\right)(1 - 2s)}{3a^{*4}G^*} \tag{44}$$

On integrating it to get the quantitative plot of the lateral migration velocity with respect to time in the case of viscoelastic migration,

$$\frac{160\lambda V_{\max}^{*3}\kappa^5\left(\frac{1}{3} + \epsilon_1\right)}{3a^{*4}G^*}(ln\frac{1 - 2s}{1 - 2s_0}) = (t - t_0) \tag{45}$$

$$\frac{80\lambda V_{\max}^{*}k^3\left(\frac{1}{3} + \epsilon\right)}{-3a^{*3}}(x - x_0) = \left((s - s_0)^2 - (s - s_0) - \frac{1}{2}\log\left(\frac{2s - 1}{2s_0 - 1}\right)\right) \tag{46}$$

Equation (45) gives the lateral position s as a function of time, while equation (46) gives the lateral position with respect to the axial position in the flow domain. These plots in Figure 3 and 4 helps us to analyse the lift in second order fluids, both temporally and also with respect to axial position. The predicted results do agree qualitatively with the trajectories measured in 3-D poiseuille flow also, for the certain constant parameters such as $\lambda > 0$ and $\epsilon_1 = -0.55$.The main feature of interest for Poiseuille flow, which we shall discuss at greater length in the following section, is the skewness of the trajectories in the sense that spheres near the wall clearly migrate more rapidly than those near the centre for a given average flow rate in a given fluid. This feature reflects the larger lateral force associated with the region nearest the wall.

Hence, as κ is increased, the migration of particles from the wall towards the 'equilibrium' position is more effective than the migration from the region nearer the centre-line, and the steady-state concentration distribution becomes skewed in favour of more particles in the centre and less near the walls. Thus, initially the change in μ_{app} is towards lower values as the decrease in dissipation due to migration away from the walls dominates the increase caused by outward migration from the vicinity of the centre-line. Finally, the reason for t and x to be scaled is due to the lateral migration is very less compared to the axial position and time marching.

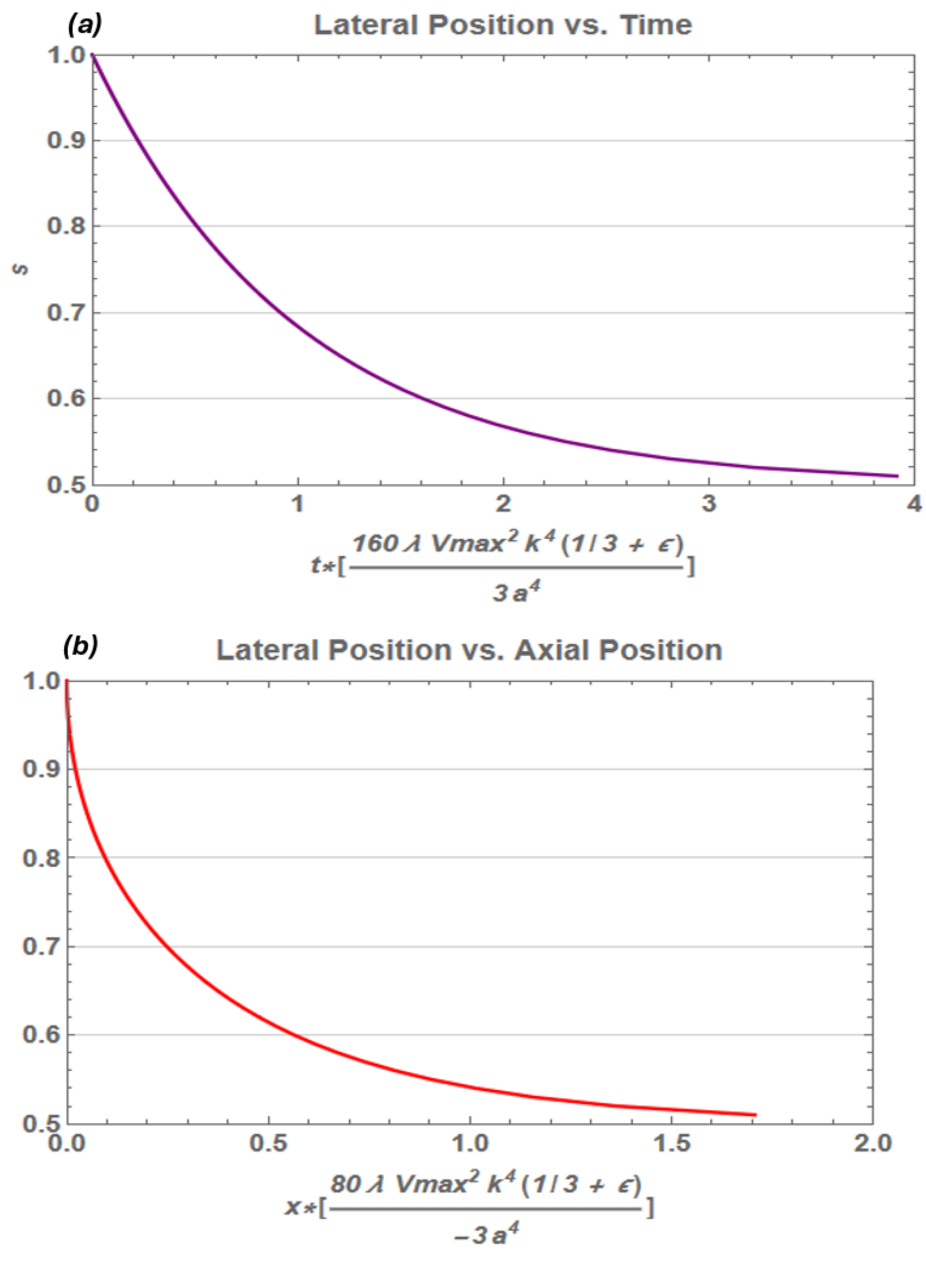

Figure 3: 2. Particle trajectory for two-dimensional Poiseuille flow : lateral position v/s (a) time and (b) axial position. **Parameters used:**$\kappa = 0.017, V^*_{max} = 2.9 * 10^{-3}, a = 1.1 * 10^{-6}, \lambda = 0.12$

These two plots above are only for particle in viscoelastic flow (in second-order fluid) and till now we have consider the particle to be neutrally buoyant and no external electric field is acting as of now.

5.1 Comparison of a phorectic particle and sedimenting particle

For the evaluation and validation of the particle trajectories herw we have considered numerical analysis for all the three cases i.e., Viscoelastic Migration, migration of an electrophoretic particle under an externally applied electric field and then buoyancy influenced forced migration of a particle. The ratio of migration velocity to the translational velocity is:

$$\frac{U_{\mathrm{mig}}}{U_{\mathrm{sx}}} = \frac{ds/dt}{dx/dt} = \frac{ds}{dx}. \tag{47}$$

At the leading order, U_{sx} can be approximated as $U_{\mathrm{sx}(0)}$ because the corrections arrive at $\mathcal{O}(\lambda)$ (due to weak non-Newtonian effects) and $\mathcal{O}(\kappa^2)$ (due to wall-induced viscous resistance). Here, U_{mig} has hydrodynamic (i.e., U^H_{mig}). Using the first-order Euler method and substituting U^H_{mig} and $U_{\mathrm{sx}(0)}$, we obtain the equation governing the particle trajectory.

For viscoelastic Migration in a second order fluid:

$$\frac{U^H_{\mathrm{mig}}}{U^{(0)}_{\mathrm{sx}}} = \frac{\lambda\left(\frac{10\pi}{3}(4(1-2s))\gamma(1+3\epsilon)\right)}{6\pi\left(4\frac{s(1-s)}{\kappa} + \frac{\gamma}{3}\right)} \tag{48}$$

For an electrophoretic particle under external electric field applied parallel to the flow:

$$\frac{U^H_{\mathrm{mig}}}{U^{(0)}_{\mathrm{sx}}} = \frac{\lambda\left(\frac{10\pi}{3}(4(1-2s))\gamma(1+3\epsilon) - \left(\frac{3\pi}{2}\right)(4(1-2s))Ha\,\xi p(1+\epsilon)\right)}{6\pi\left(4\frac{s(1-s)}{\kappa} + \frac{\gamma}{3} + Ha\,\xi p\right)} \tag{49}$$

and Finally, for forced migration of a non-neutrally buoyant particle sedimenting in a second-order quescent fluid:

$$\frac{U^H_{\mathrm{mig}}}{U^{(0)}_{\mathrm{sx}}} = \frac{-\lambda\left(\frac{\pi}{3}(4(1-2s))(9\mathcal{B} - 10\gamma)(1+3\epsilon)\right)}{6\pi\left(4\frac{s(1-s)}{\kappa} + \frac{\gamma}{3} + \mathcal{B}\right)} \tag{50}$$

Using the first-order Euler method and substituting U^H_{mig} and $U_{\mathrm{sx}(0)}$, we obtain the equation governing the particle trajectory:

$$S^{n+1} \approx S^n + \Delta x\left(\frac{U^H_{\mathrm{mig}}}{U_{\mathrm{sx}(0)}}\right) \tag{51}$$

Substituting the equations (48-50) we can get the particle trajectory easily.On plotting the functions for both particle leading and lagging the flow and comparing the phoretic particle case with the sedimenting particle and analysing from the results, we observe that, in Poiseuille flow, the effect of electrophoresis on the inertial migration (phoretic-lift) is qualitatively similar to that of a non-neutrally buoyant particle i.e. a particle leading the flow, migrates towards the region of high shear and vice versa for a lagging particle. Therefore, it is of interest to find the fundamental differences between the two systems and we observe that there is a flip in the behaviour of the function between the electrophoretic particle and the sedimenting particle. However, it is difficult to compare the two cases because of the completely different parameters changing such as zeta potential and buoyancy number but we can obviously see the directional changes.

We can also see the skewness of both the curves with respect to the viscoelastic migration case and observe that in the buoyancy combined inertial lift we have steep slope and less curvature to that of viscoelastic migration and on the other hand there is a significant curvature in the curve for the electrophoretic particle. This may be due to the flow profiles of both the cases.

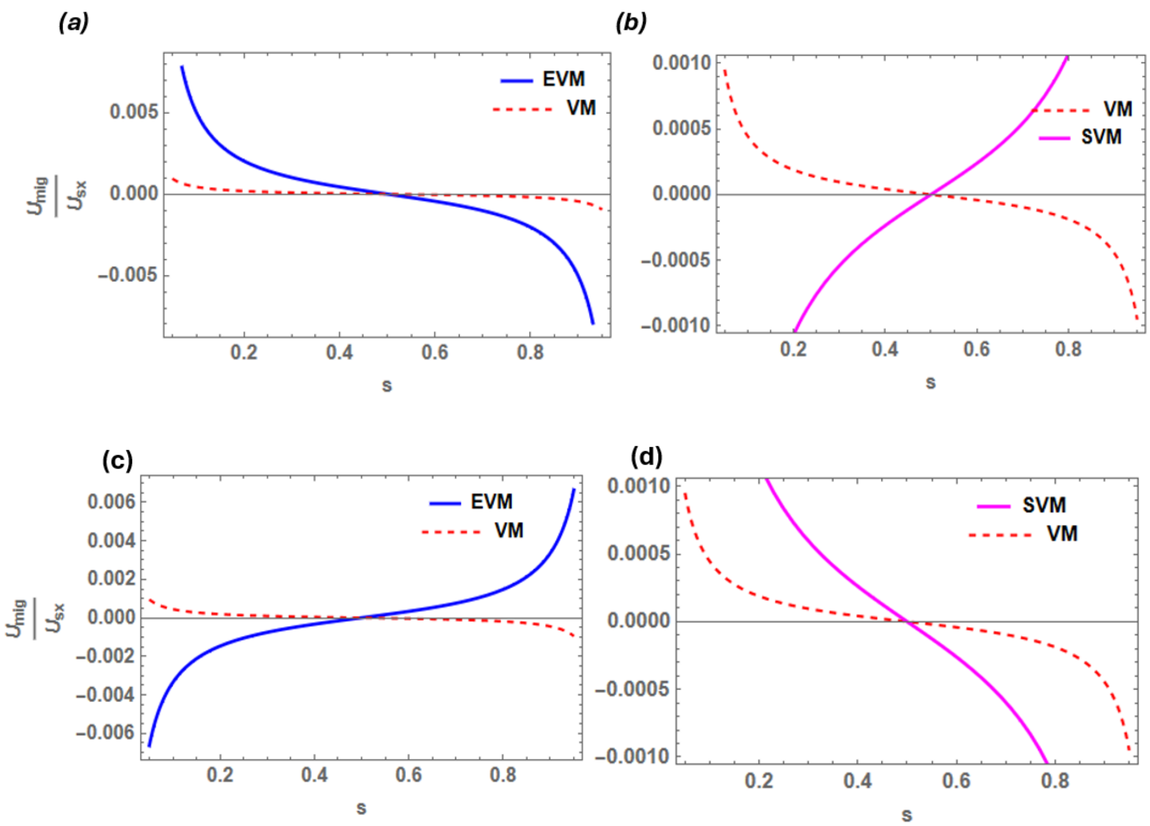

Figure 4: **(a)**It is the comparison of a electrophoretic particle wrt particle in Viscoelastic flow ($Ha = 0.8, \zeta_p = -2.52$) and **(b)** shows the behaviour of a non-neutrally buoyant particle (forced migration) wrt force-free migration in viscoelastic flow($\mathcal{B} = -0.5$),**(c)** similar to the plot (a) but it is of $\zeta_p = -2.52$ and finally **(d)** is of positive buoyancy number. *Other parameters*:$\kappa = 0.017, \lambda = 0.12, \epsilon_1 = -0.55$

6 Conclusion

Inertial Migration: For a neutrally buoyant rigid sphere in Newtonian fluids under Poiseuille flow, lateral migration arises due to inertial effects, primarily through the interaction between the stresslet and the confining walls. However, the resulting lift is weak and insufficient for significant cross-stream migration unless inertia is sufficiently high.

Viscoelastic Migration: In second-order viscoelastic fluids, even in the absence of significant inertia, particles migrate laterally due to normal stress differences. The derived lift force is directly proportional to both shear rate and viscometric parameters (λ and ϵ_1), and pushes the particle towards the centerline of the flow. This lift is of order $\mathcal{O}(\lambda\kappa^3)$ and fundamentally arises from local stress interactions near the sphere, rather than wall interactions as in Newtonian fluids.

Electrokinetically Enhanced Viscoelastic Migration: When an electric field is applied parallel to the flow, electrophoretic slip at the particle surface introduces an additional migration mechanism. The electrokinetic contribution enhances the lateral migration significantly (order $\mathcal{O}(1)$), with the lift force containing a dominant term proportional to $\mathrm{Ha}\cdot\zeta_p$. Interestingly, the migration direction is found to be opposite to that of sedimenting (forced) particles under otherwise similar flow conditions.

Forced Migration (Sedimentation): When gravity is introduced, a non-neutrally buoyant particle experiences a distinct migration behavior due to the Stokeslet-dominated disturbance field. Unlike the electrophoretic (force-free) case, the lift in sedimenting particles is driven by slower-decaying velocity fields and results in stronger lateral forces of order $\mathcal{O}(1)$.

Comparative Trajectories: Numerical simulations show that the electrophoretic and sedimenting particles exhibit contrasting lateral trajectories under identical viscoelastic conditions, despite both leading to enhanced migration. The skewness and curvature in particle paths reveal unique characteristics of phoretic vs. forced migration mechanisms, validating the theoretical predictions.

We can also visualize the trajectories more accurately by the plots of the lateral position versus the axial position. Therefore, upon using explicit euler we get the actual trajectory of all the three cases plotted in figure 5 below.The figure presents the trajectories of particles under different flow conditions, comparing the effects of electrophoretic migration and buoyancy-driven sedimentation in a viscoelastic medium. Figures 5(a) and 5(b) depict the behavior of an electrophoretic particle. The blue curves indicate that the electrophoretic particle moves differently compared to the viscoelastic migration (red curves). The viscoelastic effect tends to stabilize the particle closer to the centerline of the flow. Figures 5(c) and 5(d) show the behavior of a buoyancy-influenced sedimenting particle. The magenta curves suggest that forced migration (due to buoyancy) competes with viscoelastic migration, leading to distinct trajectories.

Since $\alpha \sim O(\kappa^{-1})$, $\gamma \sim O(\kappa)$, $Ha(\zeta_p) \sim O(1)$, the trajectory equation can be approximately represented

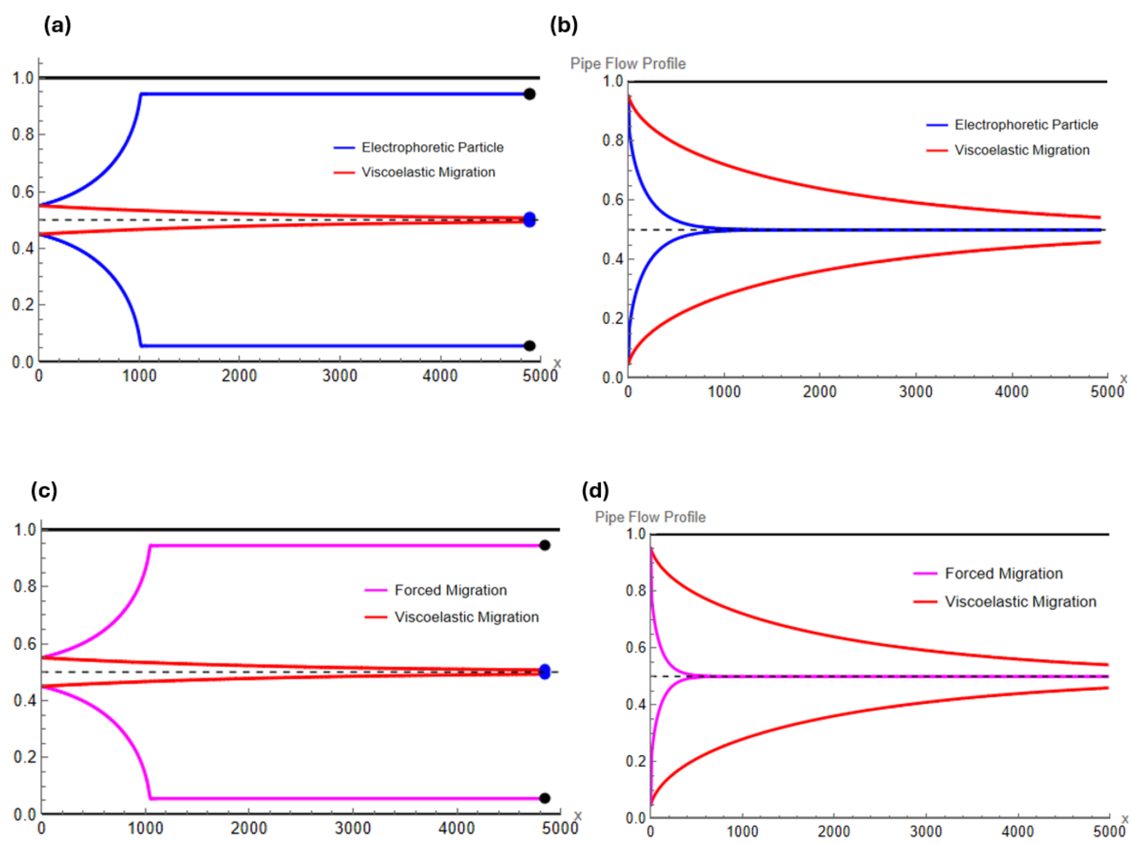

Figure 5: Plotting the particle Trajectories for both the cases (particle leading a flow and particle lagging a flow) fig 5(a and b) for electrophoretic particle and fig.5(c and d) for a buoyancy influenced sedimenting particle.

7 Future Directions

Main Objective: Finding out the reason of this weird behavior by solving the first order velocity field(flow field) and then from there find the force from conventional ways and compare the results.